water

MDPI

Article

Performance Evaluation of Small Sized Powdered Ferric Hydroxide as Arsenic Adsorbent

Muhammad Usman [1,*], Ioannis Katsoyiannis [2], Manassis Mitrakas [3], Anastasios Zouboulis [2] and Mathias Ernst [1,*]

1 Institute for Water Supply and Water Resources, Hamburg University of Technology, Am Schwarzenberg Campus 3, 21073 Hamburg, Germany
2 Laboratory of Chemical and Environmental Technology, Department of Chemistry, Aristotle University of Thessaloniki, 54124 Thessaloniki, Greece; katsogia@chem.auth.gr (I.K.); zoubouli@chem.auth.gr (A.Z.)
3 Analytical Chemistry Laboratory, Department of Chemical Engineering, Aristotle University of Thessaloniki, 54124 Thessaloniki, Greece; manasis@eng.auth.gr
* Correspondence: muhammad.usman@tuhh.de (M.U.); mathias.ernst@tuhh.de (M.E.); Tel.: +49-40-42878-3177 (M.U.); +49-40-42878-3453 (M.E.)

Received: 3 July 2018; Accepted: 18 July 2018; Published: 20 July 2018

Abstract: The small sized powdered ferric oxy-hydroxide, termed Dust Ferric Hydroxide (DFH), was applied in batch adsorption experiments to remove arsenic species from water. The DFH was characterized in terms of zero point charge, zeta potential, surface charge density, particle size and moisture content. Batch adsorption isotherm experiments indicated that the Freundlich model described the isothermal adsorption behavior of arsenic species notably well. The results indicated that the adsorption capacity of DFH in deionized ultrapure water, applying a residual equilibrium concentration of 10 µg/L at the equilibrium pH value of 7.9 ± 0.1, with a contact time of 24 h (i.e., Q_{10}), was 6.9 and 3.5 µg/mg for As(V) and As(III), respectively, whereas the measured adsorption capacity of the conventionally used Granular Ferric Hydroxide (GFH), under similar conditions, was found to be 2.1 and 1.4 µg/mg for As(V) and As(III), respectively. Furthermore, the adsorption of arsenic species onto DFH in a Hamburg tap water matrix, as well as in an NSF challenge water matrix, was found to be significantly lower. The lowest recorded adsorption capacity at the same equilibrium concentration was 3.2 µg As(V)/mg and 1.1 µg As(III)/mg for the NSF water. Batch adsorption kinetics experiments were also conducted to study the impact of a water matrix on the behavior of removal kinetics for As(V) and As(III) species by DFH, and the respective data were best fitted to the second order kinetic model. The outcomes of this study confirm that the small sized iron oxide-based material, being a by-product of the production process of GFH adsorbent, has significant potential to be used for the adsorptive removal of arsenic species from water, especially when this material can be combined with the subsequent application of low-pressure membrane filtration/separation in a hybrid water treatment process.

Keywords: arsenic adsorption; small sized powdered ferric hydroxide; granular ferric hydroxide; water matrix; adsorption kinetics; drinking water

1. Introduction

Arsenic is globally considered as one of the major pollutants in drinking water sources and a worldwide concern because of its toxicity and carcinogenicity [1]. The presence of arsenic at elevated concentrations in natural environments can be attributed to both natural and anthropogenic inputs [2]. Arsenic pollution is primarily caused by natural processes, such as the weathering of rocks and minerals, followed by leaching and industrial activities that lead to the pollution of soil and

groundwater [3]. The discharge of arsenic polluted waters from mining or mining-related activities, the pharmaceutical industry and agricultural activities plays an important role in anthropogenic arsenic pollution in Asia [4]. However, the introduction of arsenic into groundwaters is expected to occur mainly as a result of its natural geological presence in rocks [5].

Arsenite As(III) and arsenate As(V) are considered as the main oxidation states of inorganic arsenic found in natural waters. As(V) anions are predominant and stable in oxygen-rich environments, whereas the As(III) anions prevail in moderately reduced environments (i.e., anaerobic or anoxic groundwaters). Therefore, arsenic speciation mostly depends on pH and redox potential (Eh) conditions. Under oxidizing conditions and at pH values relevant to drinking water treatment, H_3AsO_4 is present as an oxyanion in the forms of $H_2AsO_4^-$ and/or $HAsO_4^{2-}$, whereas at low Eh values, arsenic becomes dominant as H_3AsO_3. Up to pH 9, H_3AsO_3 does not dissociate and, therefore, is present in most natural waters as the uncharged arsenious acid [6]. Therefore, As(III) species are considered as much more mobile in aquifers and cannot be easily adsorbed (and removed) onto the usually co-existing mineral surfaces, such as those of iron oxides. Moreover, As(III) is more toxic for the biological systems, as compared to As(V) [3,7].

The pollution of drinkable water sources by arsenic has been reported in more than 70 countries, where more than 150 million inhabitants are under high health risk [8]. Due to its high toxicity to humans, the World Health Organization [9] lowered the guideline value for arsenic in drinking water from 50 to 10 μg/L in 2004, aiming to minimize the health-related problems associated with arsenic pollution. The same standards also apply in the European Commission, as well as the US Environmental Protection Agency. Among other countries, the arsenic pollution of groundwater is considered as a particularly serious health-related problem in Pakistan, as a recent survey reveals [10]. Approximately 50 to 60 million people relying on groundwater as a source of drinking water in the Indus Valley are at high health risk [11]. In Punjab, more than 3% of the inhabitants are exposed to arsenic concentrations higher than 50 μg/L in drinking water, and 20% of the population is exposed to concentrations higher than 10 μg/L, while 16% and 36% of inhabitants in Sindh areas are exposed to arsenic pollution of concentrations higher than 50 μg/L and 10 μg/L, respectively [10].

Several treatment technologies to remove arsenic from drinking water have been applied worldwide [12], including adsorption using activated alumina [13] or iron oxide-based adsorbents, such as tetravalent manganese feroxyhyte [14], bayoxide [15–17], granular ferric hydroxide (GFH) [18], etc. Other treatment methods include the application of oxidation and arsenic removal using zero-valent iron (especially in Bangladeh) [19], coprecipitation of arsenic with iron or aluminum salts [2], preliminary arsenic oxidation by ozonation or biological oxidation [19], ion exchange [20], high pressure membrane separation [21,22] and electrocoagulation [23]. According to Tresintsi [14], chemical precipitation by ferric coagulation has significantly higher arsenic removal efficiencies in comparison to adsorption by iron oxy-hydroxides, and a drinking water regulation limit can be achieved at an affordable price, with operational costs estimated between 0.09 and 0.16 €/m^3 for initial arsenic concentrations, ranging between 19 and 208 μg/L. However, the major part (>90%) of treatment costs was attributed to the management of produced sludge, since the coagulant costs are estimated to be $\leq$0.01 € [15]. Previous studies have identified high pressure membrane processes as an emerging technology, due to their high removal efficiencies and easy operation features [21,22], but these high pressure membrane processes are rather energy (and cost) intensive, and subjected to the fouling of membranes. Moreover, the disposal of produced brine (high salt concentrations) is a considerable challenge.

On the other hand, for the treatment of waters with moderate arsenic concentrations, i.e., slightly higher than the regulation limits, adsorption onto iron oxide-based adsorbents has been proved to be the most economically efficient procedure [15]. The two mostly commercially applied adsorbents are the Granular Ferric oxy-Hydroxides (GFH) and the Bayoxide E33 (GFO), which are favorable in terms of cost, removal efficiency, simplicity of design, operation, maintenance and minimizing the (secondary) waste production [24]. The GFH has been tested to remove arsenic from

drinking water sources under both laboratory-scale and full-scale water treatment plants [15,18,25,26]. Arsenic adsorption onto GFH is usually performed in a column filtration mode, which is a rather simple process and can be continuously operated, but the production of this material is relatively cost intensive. The cost (on dry basis) for GFH and Bayoxide materials was estimated to be 9 €/kg and 12.5 €/kg, respectively [15]. Currently, the small sized fraction (dust ferric hydroxide, DFH) generated during the industrial production of GFH cannot be employed in the common column filtration mode, since the small sized adsorbents can rapidly clog the fixed beds in filter columns, causing an increased pressure head, thereby increasing energy costs and maintenance and, hence, reducing the system performance.

Adsorption combined with the application of low-pressure membrane filtration is considered as a newly developed hybrid water treatment process. Low-pressure membrane processes, such as microfiltration or even ultrafiltration, have a reasonable energy demand and produce superior quality treated water with a rather controllable fouling of membranes and incurring quite low capital and operational costs [27]. The low-pressure membrane processes are not able to remove mono- and polyvalent ions, i.e., arsenic species, from water sources, although they can efficiently remove suspended solids, colloids, bacteria, viruses and micro-particles [28]. If the cost-effective small sized GFH adsorbent (having a substantially lower commercial price of only 1.6 €/kg on a dry basis) has the potential to remove arsenic species from drinking water sources, it might then be employed in the adsorption-microfiltration (MF) hybrid treatment scheme to economically and efficiently remove arsenic. The idea of a submerged membrane filtration adsorption hybrid system could be exploited in this regard, which allows the pollutant to be in contact with adsorbents for longer time.

The objectives of the study were: (i) To assess the adsorption potential/performance of the smaller fraction of GFH material with a particle size of <0.250 mm, which is abbreviated as DFH henceforth, for removing As(V) and As(III) species from different water matrixes; (ii) to determine the kinetics of arsenic adsorption on the studied material; (iii) to examine the effect of a water matrix on arsenic removal; and (iv) to compare the efficiencies of both major inorganic arsenic species, As(V) and As(III), with the established, conventionally applied adsorbents, such as GFH. Badruzzaman [29] studied the use of small sized GFH in packed bed columns, but investigated the adsorption potential of this material only in the case of As(V) and ultra-pure water and has found promising results. However, to the best of our knowledge, no comprehensive study concerning the application of DFH material, systematically studying the arsenic adsorption efficiency of both arsenic species and different water matrices, such as the tap water of Hamburg (HH tap water) and the NSF (National Sanitation Foundation) challenge water, used to simulate typical arsenic-containing groundwater, has yet been performed.

2. Materials and Experimental Methods

2.1. Reagents

For the preparation of As(III) or As(V) 100 mg/L stock solutions, the standard solution of As(III), as As_2O_3 in 2% HNO_3, and As(V), as H_3AsO_4 in HNO_3, with a concentration of 1 g/L, were used, obtained from Carl Roth GmbH + Co. KG (Karlsruhe, Germany) and Merck Chemicals GmbH (Darmstadt, Germany), respectively. The pH buffer solution, *N*,*N*-Bis-(2-hydroxyethyl)-2-aminoethane sulphonic acid (BES), used in the experiments focusing on arsenic removal from deionized (DI) water, was obtained from Carl Roth GmbH + Co. KG.

2.2. Material Characterization

The DFH material, with a particle size of <0.250 mm, was supplied by GEH–Wasserchemie GmbH & Co. KG, Osnabrück, Germany. The material is predominantly akaganeite, a specific form of an iron oxy-hydroxide [16]. DFH is mainly characterized by a relatively large specific surface area (252 m^2/g) [29] and surface charge density (Table 1).

Table 1. Main properties of used DFH material.

Properties	Value	Literature Value
Chemical composition	β-FeOOH and Fe(OH)	
Dry solids content (%)	~50 [a]	~50 [b]
Moisture content (%)	~50 [a]	~50 [b]
Particle size (μm), d_p	7.4–250 [a]	1.8–250 [b]
Mean particle size (μm)	78.40	–
Point of zero charge (PZC)	5.3 ± 0.2	~5.5 [c]
Isoelectric point (IEP)	7.8 ± 0.2	~7.8 [c]
Surface charge density	0.9 mmol $[OH^-]$/g	–

Note: [a] Average values from triplicate analysis, [b] Data by Ref. [29], [c] Data by Ref. [30].

Particle size distribution was determined by EyeTech™ instrument (combi, AmbiValue, Nijerdal, The Netherlands), ranging between 7.4 and 250 μm. The liquid flow cell of EyeTech was filled with 1 L of deionized water, and approximately 100 mg of material was added. Mechanical shaking was provided in the liquid flow cell, which keeps the material particles in suspension. Then, suspension was supplied to the optical cell and circulated through it for 5 min at a pump speed of 0.674 L/min. Three cycles of the suspension were performed to determine the particle size distributions.

To determine the surface charge of DFH in the suspension, the Isoelectric Point (IEP) and the Point-of-Zero Charge (PZC) were quantified. IEP was determined by a zeta-potential curve at 20 ± 1 °C of adsorbent dispersion in 0.01 M $NaNO_3$, with the respective pH of solution, using a Micro-electrophoresis Apparatus (Mk II device, Rank Brothers Ltd, Cambridge, England), while PZC and the surface charge density were defined by the application of acid/base potentiometric mass titration in suspensions of the adsorbent and for various ionic strengths [31].

2.3. Water Matrix

The test solution was initially prepared using deionized water (DI), spiked with either As(III) or As(V) species, at an initial concentration of 190 μg/L. 2 mM of *N*,*N*-Bis(2-hydroxyethyl)-2-aminoethanesulfonic acid (BES) was added to the test solution, made of DI water, for pH control at pH 7.9. In addition to DI water, As(V) and As(III) test solutions were prepared in HH tap water and NSF water with the same initial arsenic concentration, as used in the case of DI water, in order to study the effect of different water matrixes on the arsenic adsorption capacity. The major physicochemical parameters of the HH tap water and of NSF challenge water are listed in Table 2.

Table 2. Water quality parameters of Hamburg tap water (* data obtained from Hamburgwasser) and NSF challenge water.

Parameter. (mg/L)	Water Matrixs.	
	HH Tap Water *	NSF Challenge Water
Na^+	14	73.7
Ca^{2+}	42	40.1
Mg^{2+}	4	12.6
HCO_3^-	150–300	183.0
Cl^-	19	71.0
SO_4^{2-}	23	50.0
NO_3^-	0.62	2.0
F^-	0.13	1.0
PO_4^{3-}	0.05–0.15	0.123
SiO_2	16.6–18.5	20
DOC	0.8 ± 0.2	–

The NSF challenge water was prepared according to the National Sanitation Foundation (NSF) international and contains the following: 252 mg $NaHCO_3$, 12.14 mg $NaNO_3$, 0.178 mg $NaH_2PO_4 \cdot H_2O$, 2.21 mg NaF, 70.6 mg $NaSiO_3 \cdot 5H_2O$, 147 mg $CaCl_2 \cdot 2H_2O$ and 128.3 mg $MgSO_4 \cdot 7H_2O$ in 1 L of DI water. Prior to adsorption experiments, the pH was adjusted to 7.9 by adding either NaOH or HCl standard solutions (0.1 N) [32].

2.4. Batch Adsorption Procedure

Batch equilibrium and kinetic adsorption tests were performed to study the adsorption potential of DFH for removing arsenic species from the different examined test solutions/water matrixes. To derive the adsorption isotherms, the method of adding various quantities of adsorbent to a constant solution volume (500 mL), having the same initial concentration of As(V) or As(III) species, was adopted. Additionally, As(III) test solutions were preliminary bubbled for 30 min with pure N_2 gas at 0.1 bar (flowrate 11.25 mL/min) to minimize the influence of dissolved oxygen on As(III) potential oxidation and adsorption, and the flasks were immediately closed and placed on the platform shaker in darkness in the thermostate cabinet (20 ± 0.5 °C) to insure the stability of As(III) species during and after adsorption onto the examined iron oxide-based adsorbents.

The evaluation of the examined adsorbent material focused on its ability to decrease the residual arsenic concentration below the drinking water regulation limit of 10 μg/L (termed Q_{10} hereafter), rather than studying the (more convenient) maximum capacity (Q_{max}) at higher residual arsenic concentrations. If efficiency of the adsorbent was evaluated through Q_{max}, which usually points to high residual concentrations and, indeed, brings high adsorption capacities, but provides marginal information on its ability to reach low concentrations, such as the regulation limits [33].

Different adsorbent dosages were placed in flasks for the three different water matrixes, while only adsorbent dosages, ranging between 5–40 mg/L, 6–50 mg/L and 10–80 mg/L, provided equilibrium As(V) concentrations between 1 and 120 μg/L in DI water, HH Tap water and NSF water, respectively. Adsorbent dosages of 10–60 mg/L, 15–100 mg/L and 40–200 mg/L were found to provide the same range of equilibrium concentrations in the experiments focusing on the removal of As(III) in DI water, HH Tap water and NSF water, respectively. For comparison, batch adsorption isotherm studies were also conducted with the GFH material, using DI water to compare the adsorption characteristics of GFH with those obtained when using DFH, i.e., to examine the efficiency of both particle size fractions of this adsorbent. GFH dosages, ranging between 10–80 and 20–120 mg/L, were carefully placed in flasks for the removal of As(V) or As(III) species, respectively. For each experimental test focusing on adsorption isotherm, a reference blank sample (i.e., without the presence of an adsorbent) was filled. The flasks were stirred using a platform shaker for 24 h at 20 ± 0.5 °C. The equilibration time was determined for the corresponding kinetic experiments. At the end of the equilibration time, the suspensions were immediately filtered through a 0.45 μm membrane syringe filter (PVDF, Carl Roth GmbH + Co. KG), and the filtrates were collected and stored for the subsequent analytical determination of residual (still dissolved and removed) arsenic.

In the kinetic studies, the initial arsenic concentration and adsorbent quantity was kept at 190 μg/L and 50 mg/L, respectively. The initial concentrations of either only As(V) or only As(III) species were the same as in the respective isotherm studies. Batch adsorption kinetics tests were conducted at the initial pH value of 7.9. Unlike the isotherm studies, a magnetic stirrer (100 rpm) was used in the kinetic studies experiments. The samples were collected at regular time intervals and the residual arsenic in the solution was analyzed. Each set of adsorption batch isotherm and kinetics experiments was replicated at least twice, and the average values are reported.

2.5. Chemical Analytics

Initial and residual arsenic concentrations were determined by Graphite Furnace Atomic Absorption Spectrophotometry (Perkin-Elmer 4100ZL, Baesweiler, Germany), using a Perkin-Elmer 4100ZL instrument [34]. The limit of detection was 0.5 μg/L. Prior to analysis, As(III) water samples

from the isotherm experiments were acidified (2 < pH < 4) and passed through a 30 mL column (with ID = 2 cm), containing an anion exchange resin (Dowex® 1 × 8–100, mesh size 50–100, Sigma-aldrich Chemie GmbH, Taufkirchen, Germany), which retained As(V), whereas the total arsenic concentration of water samples from the adsorption kinetics experiments were analyzed. This method of arsenic speciation needs approx. 50 mL of water sample, noting that, in the kinetics experiments, only small volumes (~7 mL) of water samples were collected at regular intervals; accordingly, arsenic speciation using this method was not possible. Therefore, only the total arsenic concentration of the water samples from adsorption kinetics was analyzed, presenting the concentration of individual arsenic species in the water samples. The initial concentration of phosphate in HH tap water was measured using ICP-MS (NexION 300D, PerkinElmer, Baesweiler, Germany).

3. Results and Discussion

3.1. Particle Size Distribution

The particle size has a strong effect on the removal kinetics of arsenic. Banerjee [35] observed that the removal of As(III) by the pulverized/powdered GFH (with d_p < 63 µm) was faster than that of as-received GFH (0.320 mm < d_p < 2 mm) at same experimental conditions. A similar trend was also recorded by Tresintsi [36] during the adsorption of arsenic species onto an iron oxide-based adsorbent. The length-based and volume-based particle size distributions of DFH are shown in Figure 1a,b. The major fraction of this material has a length-based particle size ranging from 7 to less than 65 µm, while the volume-based particle size has two peaks ranging between (i) 65 and 100 µm, and (ii) 200 and 250 µm. As DFH has a constant density, the volume-based distribution gives an indication of mass distribution. The average length-based particle size of DFH particles, as determined by the EyeTech instrument, is 78.4 µm.

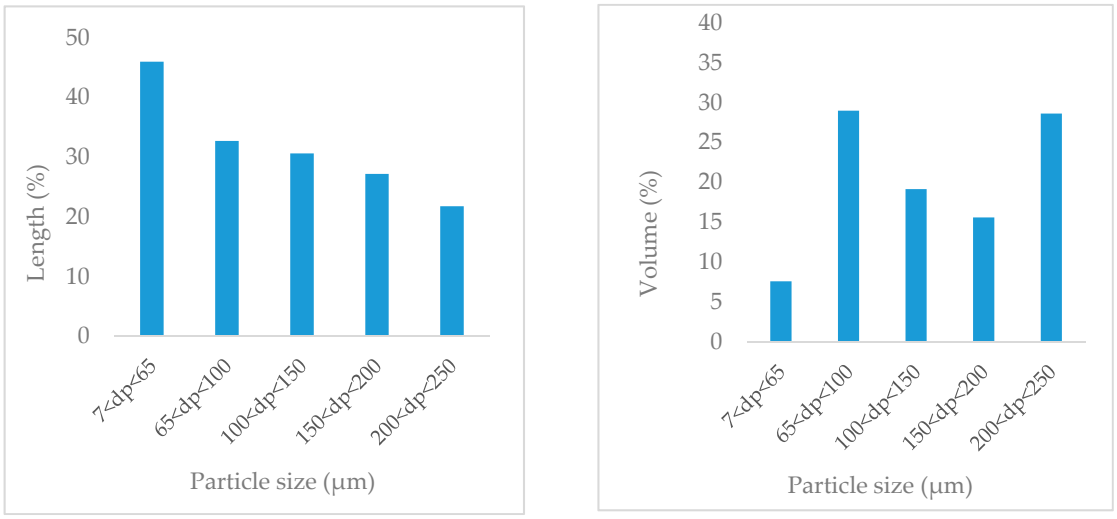

(**a**) (**b**)

Figure 1. (**a**) Length-based particle size distribution, and (**b**) volume-based particle size distribution of DFH particles, as measured by the EyeTech instrument.

Conventional GFH, which is applied in fixed bed adsorption columns (commercially available), has particle size ranging from 0.32 to 2 mm, while the particle size of tetravalent manganese feroxyhyte media, produced by Tresintsi [14] in a kilogram-scale continuous process, is of non-uniform size. A fine fraction of adsorbent media (with a particle size of <250 µm) is also generated during its production at the kilogram-scale in a laboratory two-stage continuous flow reactor.

3.2. Batch Isotherm Studies

The batch equilibrium adsorption experiments are conducted to evaluate the adsorption potential of arsenic species onto small sized powdered ferric hydroxide (DFH). The amount of arsenic adsorbed at the equilibrium stage is calculated using the mass balance of an adsorption system:

$$Q_e = \frac{(C_o - C_e)\, V}{m}, \quad (1)$$

where Q_e is the amount of arsenic adsorbed at the equilibrium stage per mass of adsorbent, C_o and C_e are the initial and equilibrium concentrations of arsenic in the test solution, respectively; m is the quantity (mass) of the adsorbent used and V is the volume of test solution.

The non-linear form of the Freundlich and Langmuir isotherm model is used to describe the adsorption behavior:

$$Q_e = K_F\, C_e^{1/n}, \quad (2)$$

$$Q_e = Q_m \frac{K_L C_e}{1 + K_L C_e}, \quad (3)$$

where K_F and n are constants, explaining the adsorption capacity and the intensity, respectively; K_L and Q_m are the Langmuir adsorption constant and maximum adsorption capacity per unit mass of adsorbent, respectively. To identify the fitting of the isotherm model to the experimental data, a chi-squared value (χ^2, Equation (4)) was also calculated, in addition to the calculation of correlation coefficients, for the non-linear form of the isotherm model. According to Tran [37], this indicates the bias in the experimental and model results. Its value is close to zero, if the data obtained using a model are similar to the experimental data, whereas its high value indicates the high biasness between the experimental data and the model estimations.

$$\chi^2 = \sum \frac{\left(Q_{e,exp} - Q_{e,cal}\right)^2}{Q_{e,cal}}, \quad (4)$$

where $Q_{e,exp}$ is the amount of arsenic adsorbed at equilibrium, and $Q_{e,cal}$ is the amount of arsenic adsorbed as calculated from the isotherm model.

3.2.1. As(V) Adsorption

The major parameters of the Freundlich isotherm in the case of As(V), along with the correlation coefficients and the respective chi-squared values, are presented in Table 3, while the Langmuir isotherm parameters are shown in Table S15 (supplementary information). The correlation coefficients and the chi-squared values indicated that the Freundlich model described the isothermal adsorption behavior of arsenic species notably well. The R^2 of the Freundlich model was greater than 0.91 and χ^2 was less than 1 for all of the (3) water matrixes. Badruzzaman [29] also reported the fitting of the Freundlich model for small fractions of GFH with an R^2 of greater than 0.92.

Table 3. Parameters of the Freundlich isotherm for As(V), along with the correlation coefficients and the respective chi-squared values.

Water Matrix	Adsorbent	n (—)	K_F *	Q_{10} (μg/mg)	R^2	χ^2
DI water	GFH	2.03	0.68	2.1	0.960	0.136
DI water	DFH	3.10	3.25	6.9	0.991	0.117
HH tap water	DFH	3.41	3.20	6.3	0.941	0.551
NSF water	DFH	2.39	1.22	3.2	0.918	0.367

Note: * $(\mu g/mg)/(\mu g/L)^{1/n}$.

The As(V) adsorption isotherms for DFH and GFH in DI water at 20 °C, with an equilibrium pH value of 7.9 ± 0.1 after a contact time of 24 h, are shown in Figure 2a. The adsorption characteristics of the DFH and GFH in DI water were analyzed and evaluated using the Freundlich isotherm equation. The K_F value for the case of DI water was 3.25 (μg As(V)/mg DFH)/(μg/L)$^{1/n}$ and the n value was 3.10, while the corresponding K_F and n values, in the case of As(V) adsorption onto GFH in DI water, were found to be 0.68 (μg As(V)/mg GFH)/(μg/L)$^{1/n}$ and 2.03, respectively. The adsorption capacity at an equilibrium liquid phase As(V) concentration of 10 μg/L (Q_{10}) and an equilibrium pH value of 7.9 ± 0.1, produced by setting the isotherm parameters in the Freundlich model, was found to be 6.9 As(V)/mg DFH and 2.1 mg As(V)/mg GFH. At the equilibrium As(V) concentration of 10 μg/L, the adsorption capacity (Q_{10}) of DFH for As(V) was almost triple that of GFH, which is also shown in Figure 2a. However, the DFH/GFH ratio of adsorption capacity diminishes from 3.2 times to 2.4 and 2.2 times as the equilibrium As(V) concentration was increased to 50 μg/L and to 100 μg/L, respectively. Banerjee [35] also reported a higher adsorption capacity of the pulverized/powdered (particle size <63 μm) GFH during the adsorption of As(V) in comparison to the as-received GFH material (with a particle size of 0.32–2.0 mm) after a contact time of 24 h and at the equilibrium pH value of 7.0–7.5. The Q_{10} value reported by Banerjee [35] for As(V) is approximately 4 times higher for pulverized GFH compared to the as-received GFH, whereas the Q_{10} value of DFH is 3.2 times higher than the as-received GFH in the current study. These results can be considered to be in agreement, since the observed small differences are considered negligible and could be attributed to the respective difference in the initial material used, since the pulverized GFH used by Banerjee [35] presented a particle size smaller than the examined DFH in this study.

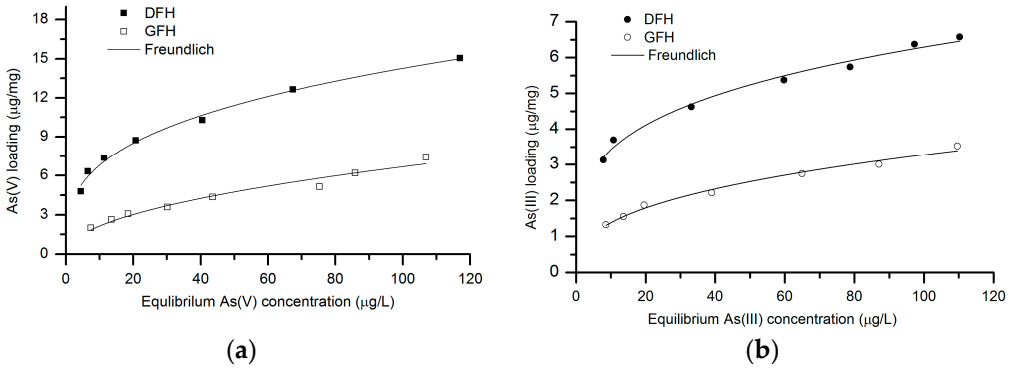

Figure 2. (**a**) As(V) and (**b**) As(III) adsorption isotherms for DFH and GFH materials in DI water. Solid lines represent the Freundlich model using non-linear fitting. Experimental conditions: Initial (As(V)) 190 μg/L, initial (As(III)) 190 μg/L, equilibrium pH value 7.9 ± 0.1 and temperature 20 °C.

In another study, Badruzzaman [29] obtained K_F (4.45 (μg As(V)/mg DFH)/(μg/L)$^{1/n}$) and n (3.57) values of a similar magnitude using the same fraction of the same adsorbent at the equilibrium pH value of 7 and 24 ± 0.5 °C after 18 days of contact time. The calculated Q_{10} value in this case was 8.5 μg As(V)/mg, which is higher than the recorded value in the current study. The divergence in Q_{10} value between the current study and Badruzzaman [29] could be ascribed to the differences of experimental conditions (equilibrium pH value, temperature, water matrix and longer contact time). At pH 7, As(V) is present as an oxyanion in the form of $H_2AsO_4^-$, while it transforms into $HAsO_4^{2-}$ at pH 8. The latter requires two active adsorption sites to be adsorbed on the absorbent surface. In addition, Badruzzaman [29] used bicarbonate as a pH buffer. In the current study, BES was used as a pH buffer to facilitate the required constant pH condition, since no influence on arsenic adsorption was observed, which is in agreement with the results reported by Banerjee [35].

In the case of granular GFH with particle sizes ranging from 0.32 to 2 mm, Banerjee [38] obtained a K_F value of 3.13 (μg As(V)/mg GFH)/(μg/L)1/n and an n value of 0.23 at the equilibrium pH of 6.5

and at 20 °C. An adsorption capacity of 5.3 μg As(V)/mg GFH is calculated by the Freundlich model, setting K_F and n values at the equilibrium liquid phase, with an As(V) concentration of 10 μg/L.

3.2.2. As(III) Adsorption

The adsorption capacity of DFH in the case of As(III), which is also higher than that obtained by the commercially-used GFH material, is shown in Figure 2b. The calculated Q_{10} value in DI water, under experimental conditions similar to As(V) adsorption isotherm experiments, was 3.5 μg As(III)/mg DFH (Table 4). Consequently, the Q_{10} value for As(III) was almost half of the corresponding value for As(V). The difference in the adsorption efficiencies between As(V) and As(III) could be attributed to the different behavior of arsenic species at the equilibrium pH value, because at pH 8, As(V) species predominantly exist as $HAsO_4^{2-}$ in aqueous solutions, while As(III) species predominantly exists as undissociated H_3AsO_3 (pKa = 9.2). As(V) adsorption onto GFH takes place via electrostatic attraction and Lewis acid–base interactions (ligand exchange reactions) [38,39]. The higher adsorption capacity of As(V) is possibly due to As(V) presenting a greater electrostatic attraction to the charged DFH particles, as compared to the electrically neutral As(III) at circumneutral pH values. Therefore, As(V) adsorbs better onto DFH than As(III).

Table 4. Parameters of the Freundlich isotherm in the case of As(III), along with the correlation coefficients and the chi-squared values.

Water Matrix	Adsorbent	n (—)	K_F *	Q_{10} (μg/mg)	R^2	χ^2
DI water	GFH	2.66	0.58	1.4	0.985	0.01
DI water	DFH	3.96	1.96	3.5	0.987	0.023
HH tap water	DFH	4.34	1.64	2.8	0.972	0.036
NSF water	DFH	4.39	0.64	1.1	0.970	0.005

Note: * $(\mu g/mg)/(\mu g/L)^{1/n.}$

As shown in Figure 2b, DFH has a higher As(III) adsorption capacity than GFH within the investigated concentration range. In particular, the obtained Q_{10} value of DFH was 2.5 times higher, than the respective values obtained by GFH. This difference was, however, reduced to 2.1 and 1.9 times at the equilibrium As(III) concentrations of 50 μg/L and of 100 μg/L, respectively. The Q_{10} value of pulverized GFH for As(III), reported by Banerjee [35], is approximately 1.8 times higher than that obtained by the granular GFH experiments. The divergence in Q_{10} value might be attributed to difference in the initial concentration, particle size and equilibrium pH.

The results of this study can be compared with similar studies using very advanced nanomaterials to achieve efficient arsenic adsorption. The study of Bolisetty [40] shows that amyloid–carbon hybrid membranes containing 10% (by weight) amyloid fibrils indeed diminished the arsenic concentration in ultrapure water within the drinking water regulation limit, but the adsorption capacity is lower than 0.3 and 1.2 μg/mg for As(V) and As(III), respectively, and the adsorption efficiency of amyloid–carbon hybrid membranes for As(V) is almost 25 times lower than that of DFH (recorded from adsorption isotherms) and 3 times lower in case of As(III). DFH media is a by-product, otherwise useless in the water industry, and can find real scale applications in a short period of time with a rather higher adsorption capacity and lower operational costs.

3.3. Effect of Water Matrix on Arsenic Adsorption

DFH batch adsorption isotherms studies were also conducted with HH tap water and NSF water to assess the real and practical adsorption potential for removing As(III) and As(V) from drinking water. The adsorption isotherms for As(V) and As(III) onto DFH at 20 °C and at the equilibrium pH value of 7.9 ± 0.1 in three different water matrixes after a contact time of 24 h are shown in Figure 3a,b.

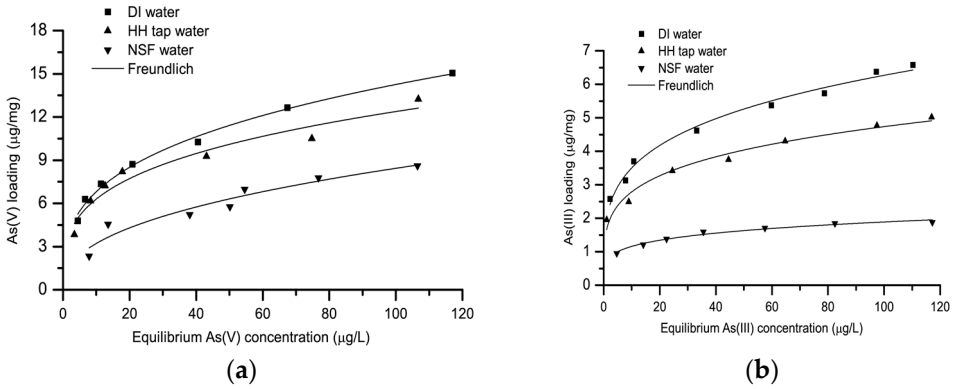

Figure 3. (**a**) As(V) and (**b**) As(III) adsorption isotherms for DFH using three different water matrixes. Solid lines represent the Freundlich model by using non-linear fitting. Experimental conditions: Initial (As(V)) 190 μg/L, initial (As(III)) 190 μg/L, equilibrium pH value 7.9 ± 0.1 and temperature 20 °C.

The adsorption capacity of DFH in HH tap water and in NSF water decreased, as compared to DI water, over the entire range of equilibrium As(V) concentrations is shown in Figure 3a. However, the decrease of the adsorption capacity was found to be more significant in the case of NSF water. For example, the Q_{10} value for As(V) in HH tap water and in NSF at the equilibrium pH of 7.9 ± 0.1 was 6.3 μg As(V)/mg DFH and 3.2 μg As(V)/mg DFH, respectively. Due to the presence of different competing interfering ions, such as phosphate and silica, the reduction of 8.2% and 53.4% in Q_{10} values for As(V) was observed regarding the cases of HH tap water and of NSF water, respectively.

In the case of As(III), the Q_{10} value of 3.5 μg As(III)/mg observed in DI water at the equilibrium pH of 7.9 ± 0.1 was reduced to 2.8 and 1.1 μg As(III)/mg in HH tap water and in NSF water, respectively. The observed reduction of Q_{10} values in the cases of HH tap water and of NSF water, can be attributed to As(III) speciation, because As(III) is electrically neutral at the set pH value of 7.9, resulting in nearly negligible electrostatic attraction, while the co-presence of their anions may have significant electrostatic attraction with the charged surface of DFH. Therefore, reductions of 20.1% and 69.0% were recorded in the Q_{10} values for As(III) in HH tap water and in NSF water, respectively, indicating also that in NSF water, the concentration of competing and interfering ions is higher, as compared with HH tap water.

Especially, the presence of phosphates and silicates showed the most adverse effect on the arsenic adsorption capacity of iron-based adsorbents [41,42]. At pH 8.2, GFH has a strong affinity with phosphate, existing as HPO_4^{2-} [43], and strongly competes with arsenic species for similar adsorption sites. Amy [16] reported a reduction of 3% in the As(V) adsorption capacity of GFH in the presence of only 125 μg/L phosphate at pH 8 during batch tests. However, the reduction of the Q_{10} value increased to 36% when the phosphate concentration was increased to 250 μg/L. In the case of silica competition under the same experimental conditions, Amy [16] reported a reduction of 25% and 60% in the Q_{10} values for As(V) when silica was present with 13.5 and 22 mg/L concentrations, respectively. During the adsorption of As(V) onto tetravalent manganese feroxyhyte (TMF) in batch adsorption tests at the equilibrium pH of 8, the measured Q_{10} values of 10.3 μg As(V)/mg and 10.9 μg As(III)/mg in DI water were reduced to 5.4 μg As(V)/mg and 4.6 μg As(III)/mg in the case of NSF water, resulting in reductions of 47.6% and 57.8% for As(V) and As(III), respectively [14]. In the case of arsenic adsorption onto Bayoxide in NSF water, Amy [16] reported reductions of 54.6% and 96.9% at the equilibrium pH of 7.5 for As(V) and As(III), respectively. Silicate also presents strong competition with arsenic species for similar adsorption sites because it exists as $H_3SiO_4^-$ at pH 8, which requires one active site for adsorption [44].

3.4. Arsenic Removal Kinetics

The rate adsorptions of As(V) and As(III) onto DFH in three different water matrixes, at 20 °C and an initial pH of 7.9, respectively, are shown in Figure 4a,b. First-order and second-order kinetic models were considered to analyze the removal rates of As(V) and As(III) from these aqueous solutions. Banerjee [38] used the first-order kinetic equation to study the adsorption of arsenic species onto GFH, while Eljamal [45] and Saldaña-Robles [46] employed the second-order kinetic equation for the adsorption of As(V). The simple forms of the first- and second-order kinetic models can be expressed as [38,46]:

$$\ln\left(\frac{As_t}{As_o}\right) = -k_1 t, \quad (5)$$

$$\frac{1}{As_t} - \frac{1}{As_o} = k_2 t, \quad (6)$$

$$SE = \sqrt{\left[\frac{\sum(C_e - C_p)^2}{n-2}\right]} \quad (7)$$

where As_0 is the initial concentration of arsenic species (either As(V) or As(III)), As_t is the liquid phase arsenic concentration remaining in the solution at time t, and k_1 and k_2 are the first- and second-order rate constants, respectively. C_e and C_p are the experimental and the predicted solid phase arsenic concentrations, and n is the total number of data points. The fitting of the kinetic model was determined by R^2 and by the standard error of estimation (SE, Equation (7)).

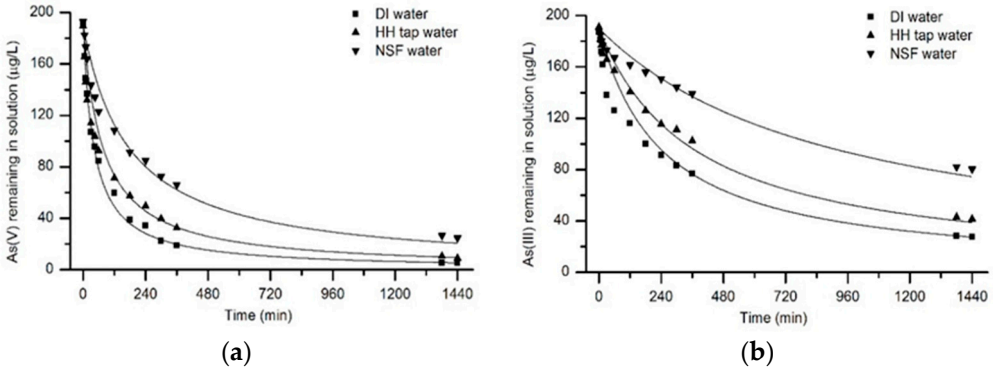

Figure 4. Rate of adsorption of (**a**) As(V) and (**b**) As(III) in different water matrixes at an initial pH of 7.9 and temperature of 20 °C, using an adsorbent dosage of 50 mg/L and an initial (As(V)) 190 µg/L and initial (As(III)) 190 µg/L.

R^2 and SE coefficients for both kinetic models, for As(V) and As(III) species, in all (3) examined water matrixes are shown in Table 5. The calculated values of SE are lower, whereas the R^2 values are higher for the second-order equation, providing a closer fit. Accordingly, the second-order kinetic model was used to further analyze the kinetics data of all water matrixes. The second-order rate constants (k_2) for As(V) and As(III) in DI water, in HH tap water and in NSF water, are presented in Table 6. The R^2 ranged from 0.992 to 0.998 and from 0.980 to 0.996 for As(V) and As(III), respectively, whereas the values of k_2 are in the range of 1.82×10^{-3} to 7.51×10^{-3} h^{-1} and of 0.34×10^{-3} to 1.34×10^{-3} h^{-1}, as calculated in the case of As(V) and As(III), respectively. The interfering ions present in the HH tap water and in the NSF water results in significantly lower k_2 values, while the lowest k_2 value was calculated in the case of NSF water.

Table 5. Correlation coefficient (R^2) for the first- and second-order kinetic models, along with the standard error of estimation (SE).

Water Matrix	As(V)				As(III)			
	First Order		Second Order		First Order		Second Order	
	R^2	SE	R^2	SE	R^2	SE	R^2	SE
DI water	0.529	59.99	0.998	4.93	0.802	35.31	0.996	14.52
HH tap water	0.579	57.62	0.994	14.31	0.769	21.59	0.969	6.72
NSF water	0.714	23.76	0.992	10.68	0.905	14.45	0.980	8.12

Table 6. Second-order rate constant (k_2) for the three examined different water matrixes.

Water Matrix	As(V)	As(III)
	k_2 (h^{-1})	k_2 (h^{-1})
DI water	7.51×10^{-3}	1.34×10^{-3}
HH tap water	4.23×10^{-3}	0.85×10^{-3}
NSF water	1.82×10^{-3}	0.34×10^{-3}

The results from batch adsorption kinetics reveal that the rate of the adsorption of As(V) onto DFH is initially fast, followed by a slower rate of adsorption, which eventually approaches an equilibrium plateau. A similar trend was observed during the adsorption of As(III) for the same experimental conditions and initial concentration of adsorbate. However, the observed uptake rate of As(III) onto DFH is slower than that of As(V), possibly because of the insignificant presence of electrostatic attraction (Coulombic interaction) in the case of As(III) adsorption [38,39]. For example, 55% and 33% adsorption of As(V) and As(III) occurred within the first 1 h of contact time, respectively, which increased up to 90% and 59% after at the end of 6 h of contact time. The slower adsorption rate of both arsenic species after 6 h of contact time can be attributed to the majority of adsorption sites, already occupied by the adsorbate species, leaving a relatively small number of adsorption sites still available for adsorption.

The results reveal that the competitive interfering ions present in HH tap water and in NSF water (in comparison with the respective experiments of DI water) can substantially reduce the removal rate of both As(V) and As(III). More specifically, the presence of interfering ions has a significant influence on the behavior of adsorption kinetics. In the case of HH tap water and NSF water, as shown in Figure 4, the strong interference of competing ions resulted in a lower adsorption rate of As(V) onto DFH, as concluded from the significant decrease of k_2 values, which decreases from 7.51×10^{-3} h^{-1} (for DI water) to 4.23×10^{-3} h^{-1} and 1.82×10^{-3} h^{-1} in the cases of HH tap water and of NSF water, respectively (Table 6). A similar negative influence, regarding the presence of phosphate and silicate ions on the As(V) adsorption rate by GFH, was also observed by Xie [41] and Nguyen [42]. Furthermore, during the adsorption of lead by iron-based adsorbents, Smith [47] also reported that the behavior of adsorption kinetics is influenced by the accessibility and availability of adsorbent surface sites, as well as by the relative surface charge, adsorbed species, and complexation rate of dissolved species with the surface sites.

4. Conclusions

In this study, the potential of a cost-effective DFH adsorbent, considered as a by-product of GFH production, for As(V) and As(III) was investigated in a systemic and detailed batch-scale study. The results show that the adsorption isotherm data obtained for As(V) and As(III) at an initial pH of 7.9 were well described by the Freundlich isotherm equation. The calculated adsorption capacity in deionized ultrapure water at the equilibrium liquid phase concentration of 10 μg/L was 6.9 and 3.5 μg/mg for As(V) and As(III), respectively. The calculated adsorption capacity of GFH at the same

pH value and equilibrium liquid phase concentration, as determined in the present study, was lower than that of DFH under the applied experimental conditions. At the equilibrium pH value of 7.9 ± 1, DFH has a considerably higher adsorbent capacity and, therefore, can bind more arsenic within the given contact time in a technical installation. However, the presence of different competing interfering ions reduces the adsorption capacity significantly, and the lowest adsorption capacity was measured in the case of NSF water that has rather elevated levels of silicate and phosphate anions. The adsorption kinetic data for both As(V) and As(III) fitted well to a second-order kinetic model. The different interfering ions of HH tap water and NSF artificial water matrixes strongly decrease the rate of uptake of As(V) and As(III), and the latter is even more greatly affected by the water matrix. To conclude, this study suggests that DFH might be successfully employed for arsenic removal from groundwaters, for example, in an adsorption-low pressure membrane hybrid system, which will be investigated in ongoing research.

Supplementary Materials: The following are available online at http://www.mdpi.com/2073-4441/10/7/957/s1, Tables S7–S14: Used adsorbent dosages for adsorption isotherm experiments. Tables S15 and S16: Langmuir isotherms parameters for arsenic adsorption.

Author Contributions: This article was written by M.U. within his PhD project. M.E. supervised the overall activities of the research project. These authors designed the research project and conducted the laboratory tests and analyses. I.K. participated in editing the paper. M.M. and A.Z. participated in the final write up.

Acknowledgments: The authors are grateful to the Higher Education Commission (HEC) of Pakistan, German Academic Exchange Service (DAAD), Greece State Scholarships Foundation and the German Society for Academic Exchanges (IKYDA), and the Technische Universität Hamburg.

Conflicts of Interest: The authors declare no conflict of interest.

References

1. Smith, A.H.; Hopenhayn-Rich, C.; Bates, M.N.; Goeden, H.M.; Hertz-Picciotto, I.; Duggan, H.M.; Wood, R.; Kosnett, M.J.; Smith, M.T. Cancer risks from arsenic in drinking water. *Environ. Health Perspect.* **1992**, *97*, 259. [CrossRef] [PubMed]
2. Violante, A.; Ricciardella, M.; Del Gaudio, S.; Pigna, M. Coprecipitation of arsenate with metal oxides: Nature, mineralogy, and reactivity of aluminum precipitates. *Environ. Sci. Technol.* **2006**, *40*, 4961–4967. [CrossRef] [PubMed]
3. Tantry, B.A.; Shrivastava, D.; Taher, I.; Nabi Tantry, M. Arsenic exposure: Mechanisms of action and related health effects. *J. Environ. Anal. Toxicol.* **2015**, *5*, 1. [CrossRef]
4. Mukherjee, A.; Sengupta, M.K.; Hossain, M.A.; Ahamed, S.; Das, B.; Nayak, B.; Lodh, D.; Rahman, M.M.; Chakraborti, D. Arsenic contamination in groundwater: A global perspective with emphasis on the Asian scenario. *J. Health Popul. Nutr.* **2006**, 142–163.
5. Garelick, H.; Jones, H.; Dybowska, A.; Valsami-Jones, E. Arsenic pollution sources. In *Reviews of Environmental Contamination*; Springer: New York, NY, USA, 2009; Volume 197, pp. 17–60.
6. Ware, G.W.; Albert, L.A.; Crosby, D.G.; Voogt, d.P.; Hutzinger, O.; Knaak, J.B.; Mayer, F.L.; Morgan, D.P.; Park, D.L.; Tjeerdema, R.S.; et al. *Reviews of Environmental Contamination and Toxicology*; Springer: New York, NY, USA, 2005.
7. Mandal, S.; Sahu, M.K.; Patel, R.K. Adsorption studies of arsenic(III) removal from water by zirconium polyacrylamide hybrid material (ZrPACM-43). *Water Resour. Ind.* **2013**, *4*, 51–67. [CrossRef]
8. Abejón, R.; Garea, A. A bibliometric analysis of research on arsenic in drinking water during the 1992–2012 period: An outlook to treatment alternatives for arsenic removal. *J. Water Process Eng.* **2015**, *6*, 105–119. [CrossRef]
9. Organization, W.H. *Guidelines for Drinking-Water Quality*; World Health Organization: Geneva, Switzerland, 2004.
10. Sanjrani, M.A.; Mek, T.; Sanjrani, N.D.; Leghari, S.J.; Moryani, H.T.; Shabnam, A.B. Current situation of aqueous arsenic contamination in Pakistan, focused on Sindh and Punjab Province, Pakistan: A review. *J. Pollut. Eff. Cont.* **2017**, *5*, 207.

11. Podgorski, J.E.; Eqani, S.A.M.A.S.; Khanam, T.; Ullah, R.; Shen, H.; Berg, M. Extensive arsenic contamination in high-pH unconfined aquifers in the Indus Valley. *Sci. Adv.* **2017**, *3*, e1700935. [CrossRef] [PubMed]
12. Hering, J.G.; Katsoyiannis, I.A.; Theoduloz, G.A.; Berg, M.; Hug, S.J. Arsenic removal from drinking water: Experiences with technologies and constraints in practice. *J. Environ. Eng.* **2017**, *143*, 3117002. [CrossRef]
13. Wang, L.; Chen, A.S.C.; Sorg, T.J.; Fields, K.A. Field evaluation of as removal by IX and AA. *J. Am. Water Work. Assoc.* **2002**, *94*, 161–173. [CrossRef]
14. Tresintsi, S.; Simeonidis, K.; Estradé, S.; Martinez-Boubeta, C.; Vourlias, G.; Pinakidou, F.; Katsikini, M.; Paloura, E.C.; Stavropoulos, G.; Mitrakas, M. Tetravalent manganese feroxyhyte: A novel nanoadsorbent equally selective for As(III) and As(V) removal from drinking water. *Environ. Sci. Technol.* **2013**, *47*, 9699–9705. [CrossRef] [PubMed]
15. Tresintsi, S.; Simeonidis, K.; Zouboulis, A.; Mitrakas, M. Comparative study of As(V) removal by ferric coagulation and oxy-hydroxides adsorption: Laboratory and full-scale case studies. *Desalt. Water Treat.* **2013**, *51*, 2872–2880. [CrossRef]
16. Amy, G.L.; Chen, H.-W.; Dinzo, A.; Brandhuber, P. *Adsorbent Treatment Technologies for Arsenic Removal*; American Water Works Association: Denver, CO, USA, 2005.
17. Ćurko, J.; Matošić, M.; Crnek, V.; Stulić, V.; Mijatović, I. Adsorption characteristics of different adsorbents and iron(III) salt for removing As(V) from water. *Food Technol. Biotechnol.* **2016**, *54*, 250–255. [CrossRef] [PubMed]
18. Thirunavukkarasu, O.S.; Viraraghavan, T.; Subramanian, K.S. Arsenic removal from drinking water using granular ferric hydroxide. *Water Sa* **2003**, *29*, 161–170. [CrossRef]
19. Katsoyiannis, I.A.; Mitrakas, M.; Zouboulis, A.I. Arsenic occurrence in Europe: Emphasis in Greece and description of the applied full-scale treatment plants. *Desalt. Water Treat.* **2015**, *54*, 2100–2107. [CrossRef]
20. An, B.; Steinwinder, T.R.; Zhao, D. Selective removal of arsenate from drinking water using a polymeric ligand exchanger. *Water Res.* **2005**, *39*, 4993–5004. [CrossRef] [PubMed]
21. Abejón, A.; Garea, A.; Irabien, A. Arsenic removal from drinking water by reverse osmosis: Minimization of costs and energy consumption. *Sep. Purif. Technol.* **2015**, *144*, 46–53. [CrossRef]
22. Víctor-Ortega, M.D.; Ratnaweera, H.C. Double filtration as an effective system for removal of arsenate and arsenite from drinking water through reverse osmosis. *Process Saf. Environ. Prot.* **2017**, *111*, 399–408. [CrossRef]
23. Nidheesh, P.V.; Singh, T.S.A. Arsenic removal by electrocoagulation process: Recent trends and removal mechanism. *Chemosphere* **2017**, *181*, 418–432. [CrossRef] [PubMed]
24. Lata, S.; Samadder, S.R. Removal of arsenic from water using nano adsorbents and challenges: A review. *J. Environ. Manag.* **2016**, *166*, 387–406. [CrossRef] [PubMed]
25. Driehaus, W.; Jekel, M.; Hildebrandt, U. Granular ferric hydroxide—A new adsorbent for the removal of arsenic from natural water. *J. Water Supply Res. Technol. AQUA* **1998**, *47*, 30–35. [CrossRef]
26. Pal, B.N. Granular ferric hydroxide for elimination of arsenic from drinking water. *Technol. Arsen. Remov. Drink. Water* **2001**, 59–68.
27. Katsoyiannis, I.A.; Zouboulis, A.I.; Mitrakas, M.; Althoff, H.W.; Bartel, H. A hybrid system incorporating a pipe reactor and microfiltration for biological iron, manganese and arsenic removal from anaerobic groundwater. *Fresenius Environ. Bull.* **2013**, *22*, 3848–3853.
28. Kalaruban, M.; Loganathan, P.; Shim, W.; Kandasamy, J.; Vigneswaran, S. Mathematical modelling of nitrate removal from water using a submerged membrane adsorption hybrid system with four adsorbents. *Appl. Sci.* **2018**, *8*, 194. [CrossRef]
29. Badruzzaman, M.; Westerhoff, P.; Knappe, D.R.U. Intraparticle diffusion and adsorption of arsenate onto granular ferric hydroxide (GFH). *Water Res.* **2004**, *38*, 4002–4012. [CrossRef] [PubMed]
30. Kersten, M.; Karabacheva, S.; Vlasova, N.; Branscheid, R.; Schurk, K.; Stanjek, H. Surface complexation modeling of arsenate adsorption by akagenéite (β-FeOOH)-dominant granular ferric hydroxide. *Colloids Surf. A Physicochem. Eng. Asp.* **2014**, *448*, 73–80. [CrossRef]
31. Kosmulski, M. *Surface Charging and Points of Zero Charge*; CRC Press: Boca Raton, FL, USA, 2009.
32. Simeonidis, K.; Papadopoulou, V.; Tresintsi, S.; Kokkinos, E.; Katsoyiannis, I.; Zouboulis, A.; Mitrakas, M. Efficiency of iron-based oxy-hydroxides in removing antimony from groundwater to levels below the drinking water regulation limits. *Sustainability* **2017**, *9*, 238. [CrossRef]

33. Simeonidis, K.; Mourdikoudis, S.; Kaprara, E.; Mitrakas, M.; Polavarapu, L. Inorganic engineered nanoparticles in drinking water treatment: A critical review. *Environ. Sci. Water Res. Technol.* **2016**, *2*, 43–70. [CrossRef]
34. Skoog, D.A.; Leary, J.J. Principles of instrumental analysis. *Clin. Chem.-Ref. Ed.* **1994**, *40*, 1612.
35. Banerjee, K.; Nour, S.; Selbie, M.; Prevost, M.; Blumenschein, C.D.; Chen, H.W.; Amy, G.L. Optimization of process parameters for arsenic treatment with granular ferric hydroxide. In Proceedings of the AWWA Annual Conference, Anaheim, CA, USA, 15–19 June 2003.
36. Tresintsi, S.; Mitrakas, M.; Simeonidis, K.; Kostoglou, M. Kinetic modeling of AS(III) and AS(V) adsorption by a novel tetravalent manganese feroxyhyte. *J. Colloid Interface Sci.* **2015**, *460*, 1–7. [CrossRef] [PubMed]
37. Tran, H.N.; You, S.-J.; Hosseini-Bandegharaei, A.; Chao, H.-P. Mistakes and inconsistencies regarding adsorption of contaminants from aqueous solutions: A critical review. *Water Res.* **2017**, *120*, 88–116. [CrossRef] [PubMed]
38. Banerjee, K.; Amy, G.L.; Prevost, M.; Nour, S.; Jekel, M.; Gallagher, P.M.; Blumenschein, C.D. Kinetic and thermodynamic aspects of adsorption of arsenic onto granular ferric hydroxide (GFH). *Water Res.* **2008**, *42*, 3371–3378. [CrossRef] [PubMed]
39. Manning, B.A.; Fendorf, S.E.; Goldberg, S. Surface structures and stability of arsenic(III) on goethite: Spectroscopic evidence for inner-sphere complexes. *Environ. Sci. Technol.* **1998**, *32*, 2383–2388. [CrossRef]
40. Bolisetty, S.; Reinhold, N.; Zeder, C.; Orozco, M.N.; Mezzenga, R. Efficient purification of arsenic-contaminated water using amyloid-carbon hybrid membranes. *Chem. Commun.* **2017**, *53*, 5714–5717. [CrossRef] [PubMed]
41. Xie, B.; Fan, M.; Banerjee, K. Modeling of arsenic (V) adsorption onto granular ferric hydroxide. *J. Am. Water Works Assoc.* **2007**, *99*, 92–102. [CrossRef]
42. Nguyen, V.L.; Chen, W.-H.; Young, T.; Darby, J. Effect of interferences on the breakthrough of arsenic: Rapid small scale column tests. *Water Res.* **2011**, *45*, 4069–4080. [CrossRef] [PubMed]
43. Genz, A.; Kornmüller, A.; Jekel, M. Advanced phosphorus removal from membrane filtrates by adsorption on activated aluminium oxide and granulated ferric hydroxide. *Water Res.* **2004**, *38*, 3523–3530. [CrossRef] [PubMed]
44. Tresintsi, S.; Simeonidis, K.; Vourlias, G.; Stavropoulos, G.; Mitrakas, M. Kilogram-scale synthesis of iron oxy-hydroxides with improved arsenic removal capacity: study of Fe(II) oxidation—Precipitation parameters. *Water Res.* **2012**, *46*, 5255–5267. [CrossRef] [PubMed]
45. Eljamal, O.; Sasaki, K.; Tsuruyama, S.; Hirajima, T. Kinetic model of arsenic sorption onto zero-valent iron (ZVI). *Water Qual. Expo. Health* **2011**, *2*, 125–132. [CrossRef]
46. Saldaña-Robles, A.; Saldaña-Robles, N.; Saldaña-Robles, A.L.; Damian-Ascencio, C.; Rangel-Hernández, V.H.; Guerra-Sanchez, R. Arsenic removal from aqueous solutions and the impact of humic and fulvic acids. *J. Clean. Prod.* **2017**, *159*, 425–431. [CrossRef]
47. Smith, E.H. Surface complexation modeling of metal removal by recycled iron sorbent. *J. Environ. Eng.* **1998**, *124*, 913–920. [CrossRef]